Direct Fiber Positioner System: A Method to Guide 50,000 Optical Fibers

Undergraduate Honors Thesis

Presented to

The Faculty of the School of Arts and Sciences

Brandeis University

Undergraduate Program in Physics

Craig Blocker and James Bensinger, Advisors

In partial fulfillment of the requirements of the degree of

Bachelor of Science

by

Kimika Arai

May 2022

Craig Blocker, Committee Member	Date
James Bensinger, Committee Member	Date

Acknowledgements

Throughout the writing of this senior thesis, I received so much support and assistance along the way. I would like to thank Craig Blocker and James Bensinger for being my thesis advisors and meeting with me every week to give me guidance and feedback. I would like to thank Kevan Hashemi for his constant support and assistance in every step of this project. Finally, I would like to thank the NSF for funding this research at Open Source Instruments. Without all of this support, this thesis could not have been written. Thank you so much.

1 Abstract

We want to build a spectroscopic telescope, which is a tool that analyzes the light of the universe. The purpose of this study is to understand the feasibility of using piezoelectric tubes (piezos) as a method of positioning 50,000 optical fibers. The goal is to precisely move and position the fibers to a given location within 10 μm, and let them stay in that position for at least one hour. However, piezos have the properties of hysteresis and creep, which makes this significantly more challenging. To combat these obstacles and gain better control of the piezos, it is necessary to learn the characteristics and quirks of the system. Therefore, this project focused mainly on understanding the behavior of the piezos under a changing voltage, as well as attempting hysteresis mitigation by experimenting with reset procedures, which, as the name implies, seeks to "reset" any memory that the system has of the previous state. Experiments showed that we can locate the fibers with a precision of 10 μm in one movement if we are experimenting with a point near the center of the system's dynamic range, and within 25 microns for other positions.

2 Introduction

2.1 Overview and Background

Important information about the universe is written in the language of lights. To decode such a language, we must perform spectroscopy, a tool to divide light into its associated energies - the electromagnetic spectrum. When analyzing an electromagnetic spectrum, one might observe spectral lines, which are essentially footprints of an atom or a molecule. Spectral lines arise due to either the excitation of an atom or when an excited atom returns to its ground state. Since each type of atom has a unique natural frequency, one can identify the kind of atom from observing the spectral lines. Astrophysicists have used this technique to understand the composition of distant stars and planets, as well as to analyze the Doppler shift of such objects. If the object is moving away from the Earth, the spectral line will appear to be red-shifted, and if the object is moving towards the Earth, the spectral line will appear to be blue-shifted [7].

Spectroscopy, since its birth and discovery, has been an important tool for astronomers and physicists alike. Today, there are still numerous mysteries of the universe that are waiting to be explained, and this could be achieved through the use of spectroscopic telescopes. For instance, the Baryon Oscillation Spectroscopic Survey (BOSS) have succeeded in producing a map of the universe containing almost one million galaxies to an accuracy of one percent [2]. This spectroscopic survey used Baryonic Acoustic Oscillations, which are fluctuations in density of baryonic matter caused by the events in the early universe. Baryonic Acoustic Oscillations were determined to be excellent standard rulers, and thus a phenomenal way to map the galactic sky.

Numerous sky surveys today have implemented multi-object spectroscopy as a part of their observation and research. The Sloan Digital Sky Survey (SDSS), which also was responsible for BOSS, conducted other surveys with success, such as Mapping Nearby Galaxies at Apache Point Observatory (MaNGA). This project utilizes a technology called the "Integral Field Units (IFUs)", as shown below.

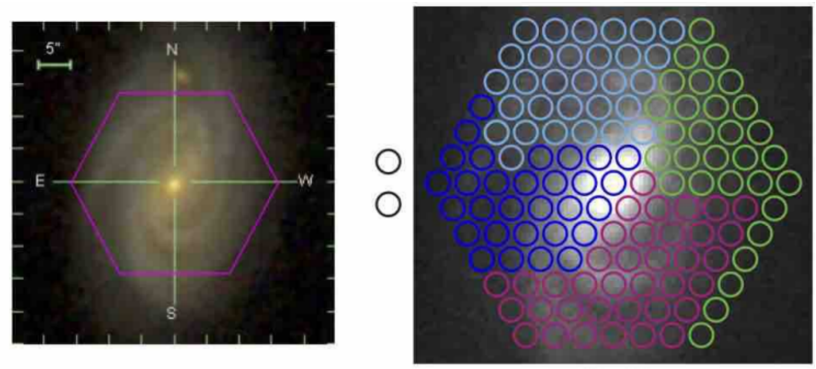

Figure 1: Example of IFU used in MaNGA. This IFU has 127 fibers on it. [5]

MaNGA uses 17 IFUs with a range of 19 to 127 fibers attached to simultaneously observe not just the centers of a galaxies, but the entire faces of galaxies. They hope to understand the entire history of these galaxies and delve deeper into their futures. Through these observations, MaNGA has been successful in producing a three-dimensional map of 10,000 nearby galaxies [1].

Another important spectroscopic experiment is the Maunakea Spectroscopic Explorer (MSE). MSE uses a tilting spine technology for its fiber positioner system, which was first used in the FMOS-Echidna (Subaru Telescope). The diagram of it is shown below.

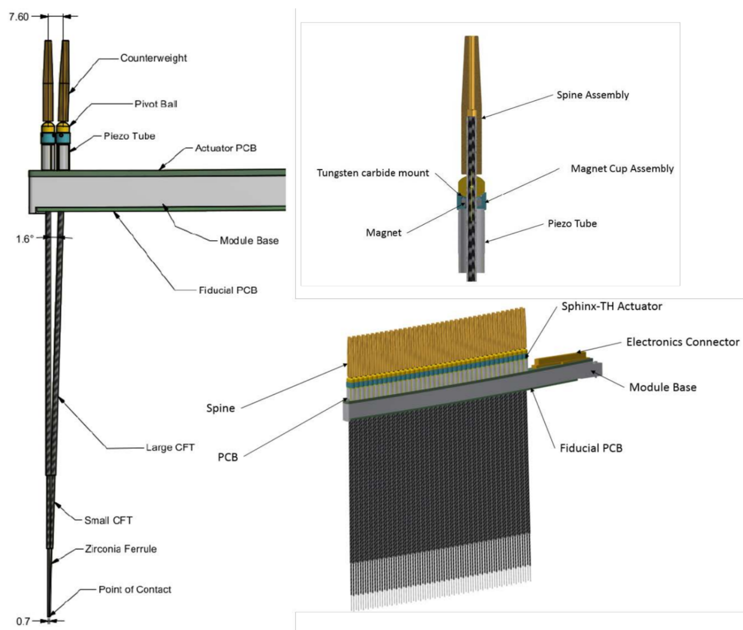

Figure 2: Fiber positioner system used in MSE. [4]

The left and the top right diagrams of figure 2 is the tilting spine technology of the MSE's fiber positioner system. There is a carbon fiber tube which forms the spine and through it there is an optical fiber together with a ferrule. The spine is positioned on top of a pivot ball and is held in place with a magnetic cup. A piezoelectric tube is beneath it all, and as a voltage is applied to the electrodes, the piezo bends, which results in a movement in the spine and hence the optical fiber, driving it to a specific position in space. The bottom right of figure 2 show that each of those Module Base carries 76 spines and the MSE has a total of 57 modules, which means that there are 4332 spines (and thus optical fibers) in this system [4].

Finally, the Dark Energy Spectroscopic Instrument (DESI) is another leading sky survey project. The instrument is located in the Nicholas U. Mayall telescope at Kitt Peak National Observatory in Arizona. A fiber positioner system is also utilized here to perform multi-object spectroscopy to produce a three-dimensional map of the universe, and a diagram of it is shown below.

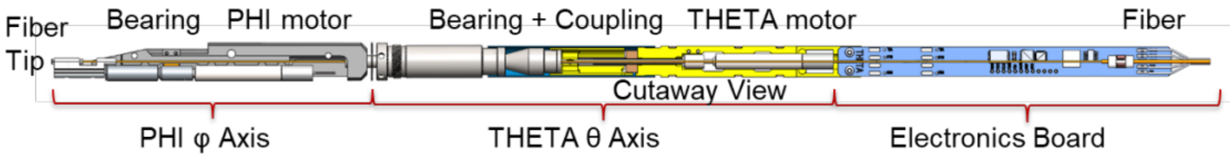

Figure 3: Fiber positioner system used in DESI. [6]

The motor in the PHI axis shown in the left of figure 3 is what positions the fibers to a given location. The motor goes through the THETA axis and is routed through the electronics board. The system is designed in such a way that a 360 degree rotation does not damage the fibers. There is a fiber view camera inside of the telescope that allows a series of iterative movements to position the fibers to a given location for an observation of the universe [6].

The three spectroscopic instruments introduced above are only few of several spectroscopy projects that are running today, or are in the works. For the future of physics and astronomy, it is necessary to continue the efforts of spectroscopic surveys, especially simultaneous, multi-object spectroscopy. These instruments could be the key to unlocking the mysteries of dark matter and dark energy that are not yet understood.

2.2 Goals for the Project

Following the community need for a spectroscopic instrument, we have done research on positioning optical fibers using piezoelectric tubes. The goal of this research project is to be able to successfully move the optical fiber to a specific, chosen location within 10 μm and let it stay there for at least one hour. Our long term goal is to have 50,000 optical fibers on the system and perform multi-object spectroscopy to further explore and understand the universe.

3 Experimental Design

3.1 Experimental Set up

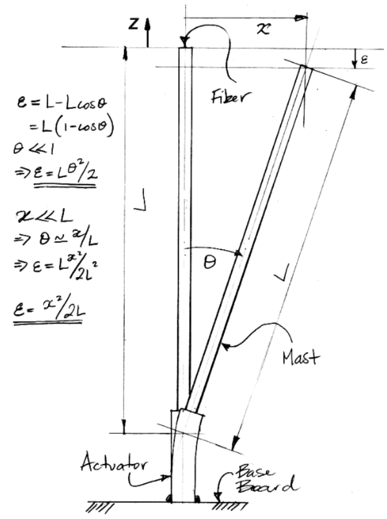

Figure 4: Experimental set up of the fiber positioner system. [3]

The experimental set up of our direct fiber positioner system consists of an optical fiber glued to a thin steel tube, and the bottom 5 mm of the thin steel tube glued into a ceramic piezoelectric tube (piezo). The piezo itself is soldered onto a circuit board that can apply a voltage to the north, south, east, and west electrodes of the piezo. When there is a voltage across the north-south electrode and/or a voltage across the east-west electrode, the piezo bends and drives the optical fiber to some location in space. A contact injector shines a light through the fiber and an overhead camera takes pictures of the fiber tip and measures its position. The camera has a charged-coupled-device (CCD), and this allows the light from the fiber to be captured when a photograph is taken and converts it to an electrical signal.

3.2 Moving the Optical Fibers

The maximum voltage one can apply to each electrode is 250 V and the minimum voltage that can be applied is -250 V. The maximum voltage across the electrodes is when there is 250 V applied to the north electrode and -250 V applied to the south electrode, as the voltage across the electrodes is simply,

$$\text{max. voltage across} = 250\text{V} - (-250\text{V}) = 500\text{V}$$

Conversely, the minimum voltage across the electrodes is when -250 V is applied to the north electrode and 250 V is applied to the south electrode. The voltage across the electrodes in this set up is,

$$\text{min. voltage across} = -250\text{V} - (250\text{V}) = -500\text{V}$$

The same applies for the voltages across the east-west electrode.

Knowing the maximum and minimum voltages that can be applied across the electrodes, we can determine the dynamic range of our system, which is graphed below.

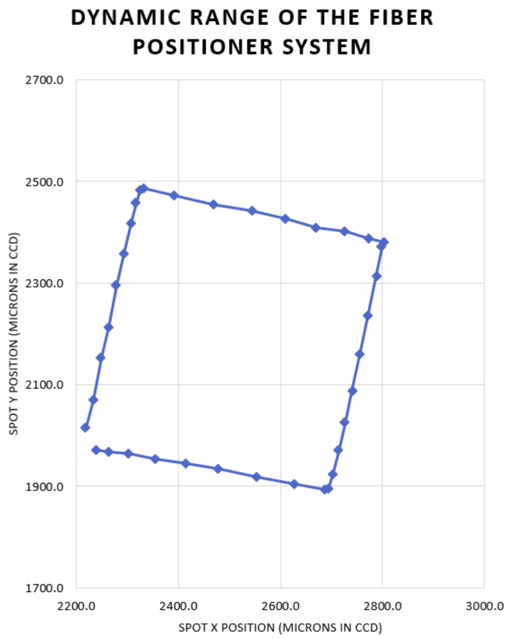

Figure 5: The dynamic range of the fiber positioner system.

Each point shown on the graph is a position of the optical fiber as it traced out the maximum range of the system. The units on the x and y axis are microns in CCD, which are the positions of the fiber as seen through the CCD camera. Experiments have shown that 1 μm on the CCD is equivalent to 6.6 μm in real space. Thus, any movement of the fiber occurs along and within the boundaries of this 3.1 mm by 3.2 mm square.

3.3 Properties of the Piezoelectric Tubes

The goal of this research project is to be able to move the optical fiber to a specific location and let it stay there for at least one hour, which is a typical observation time for astronomy experiments. While this may not sound too difficult to accomplish, the inherent properties of hysteresis and creep that the piezo possesses make this an extremely challenging project.

Hysteresis is a tendency of a material to remember its past state, which affects our system in rather troublesome ways. For example, suppose we apply 100 V to the piezo and find our optical fiber in position A. Let us then apply 50 V to the piezo and locate our optical fiber in position B. If we apply 100 V to the piezo again, we would not find our optical fiber back at position A because the piezo remembers that 50 V was applied to itself previously. This means that there is no one-to-one relationship between the voltages applied to the piezo and the position of the fiber.

Below is a graph of a hysteresis loop obtained by applying voltages across the electrodes that ramp up from -500 V to 500 V and then back down to -500 V. If the piezo did not exhibit any hysteresis, then the fiber would follow the same path when ramping up from -500 V to 500 V and ramping down from 500 V to -500 V. From the graph below, we see that this is not the case. At 0 V in the top curve, the spot x position of the fiber appears to be at approximately 1970 μm as seen on the CCD. In the bottom curve, we see that at 0 V, the fiber is at approximately 1870 μm as seen on the CCD. Therefore, we observe that there is 100 μm of hysteresis here, which is about 660 μm of hysteresis in real space.

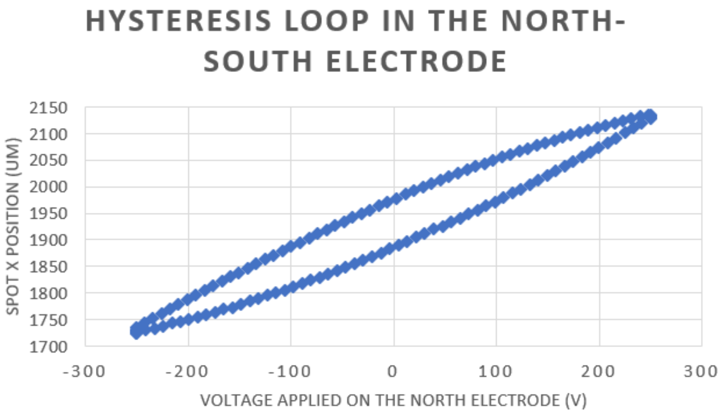

Figure 6: Hysteresis loop obtained by applying voltages that slowly increased from -500 V to 500 V and then back down to -500 V across the north-south electrode.

Moreover, creep is the change in displacement of a material under an unchanged voltage. This means that even if we succeeded in mitigating hysteresis, the fiber would continually drift from a given position under constant voltage. Without finding a method to get around both of these inherent properties, our goal can never be accomplished.

4 The Experiments

4.1 Reset Procedures

We began our study by first exploring procedures that might be able to mitigate hysteresis. Since hysteresis is a property where the material remembers its past state, it was thought that we can establish algorithms with extreme movements that can help the piezo forget where it previously was. We called these algorithms "reset procedures". We experimented with three reset procedures and the steps are described in the following subsections.

4.1.1 Diagonal Reset Procedure

The diagonal reset procedure began by applying a random voltage across the electrodes for 10 seconds. This is to model a situation where we have no idea where the fibers are initially positioned. Then we applied -500 V across the north-south electrode and the east-west electrode, and then we slowly increased the voltages across the electrodes to 500 V. Then we slowly decreased the voltages across the electrodes back down to -500 V. This pair of movement was repeated five times, and we call this step the diagonal algorithm. Then a known voltage was applied to the piezo, and the positions of the fiber was measured with an overhead camera immediately after the new voltages have been applied and after 11 seconds. This experiment was repeated over 1000 times and the final positions of the fiber were compared.

At first, we increased the voltages across the electrodes from -500 V to 500 V in one move. However, upon doing so, the fiber shook quite vigorously from the sudden, extreme movement. The shakiness is not good when attempting to measure how precisely the fiber can return to a specific position, and so we decided to slowly increase and decrease the voltages instead.

4.1.2 Spiral Reset Procedure

The spiral reset procedure also began by applying a random voltage across the electrodes for ten seconds for the same reason as above. Then we slowly spiralled the fiber to the center of its range of motion by applying the appropriate voltages across the electrodes, and we call this step the spiral algorithm. Then a known voltage was applied to the piezo, and the positions of the fiber was measured with an overhead camera immediately after the voltages were applied and after 11 seconds. Again, this experiment was repeated over 1000 times and the final positions of the fiber were compared.

4.1.3 Centered-Diagonal Reset Procedure

This final reset procedure, named the centered-diagonal reset procedure, began by first applying a random voltage across the electrodes for ten seconds. Then -500 V was applied across the north-south and the east-west electrodes. After that, 500 V was applied across both electrodes. The fiber was then moved along that diagonal such that it slowly moved towards the center. Then a known voltage was applied to the piezo, and the position of the fiber was measured with an overhead camera immediately after the voltages were applied and after 11 seconds. This experiment was also repeated over 1000 times and again, the final positions of the fiber were compared.

4.2 3 x 3 Grid Mapping Experiment

The reset procedures introduced above explored how precisely we can return the fiber tip to the same position no matter the starting voltages applied to the piezo. In this next experiment, we explored further, attempting to understand how well the fiber can return to other points along the dynamic range of the fiber positioner system.

This experiment began by first applying a random voltage across the electrodes for ten seconds. Next, we applied the spiral algorithm, and then we applied voltages across the electrodes such that the fiber moved to position one, as shown in the figure below. The position of the fiber tip was measured after waiting for 11 seconds. After that, we applied a random voltage for another ten seconds, applied the spiral algorithm, and then applied voltages such that the fiber moved to position two. This was repeated until the fiber travelled to all nine positions, and all of that was repeated another 31 times for comparison. This same experiment was repeated using the diagonal algorithm as well.

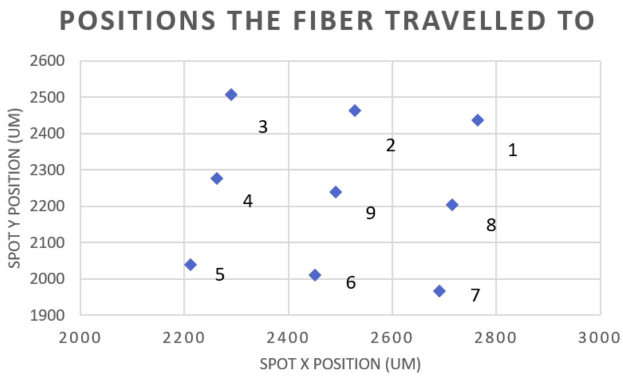

Figure 7: In this experiment, the fiber travelled to the nine positions labelled on this graph.

5 Results and Analysis

5.1 Diagonal Reset Procedure

The Diagonal reset procedure was repeated 1005 times and the final voltages applied across the north-south electrodes were 73 V and the east-west electrodes were 82 V. The final voltages applied across the voltages are the same for every trial. Below are graphs that plotted the deviations of each fiber position from the average position immediately after the final voltages were applied and after waiting for 11 seconds.

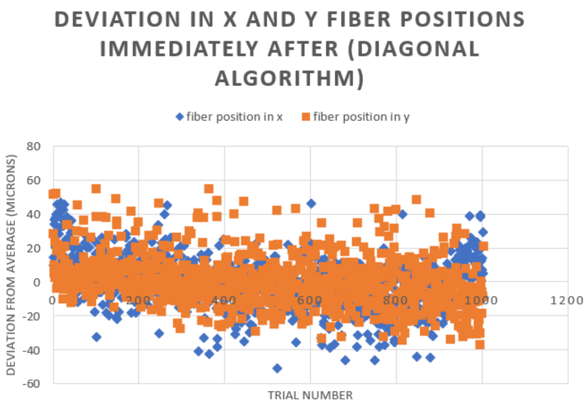

(a) Deviation from mean immediately after the voltages were applied.

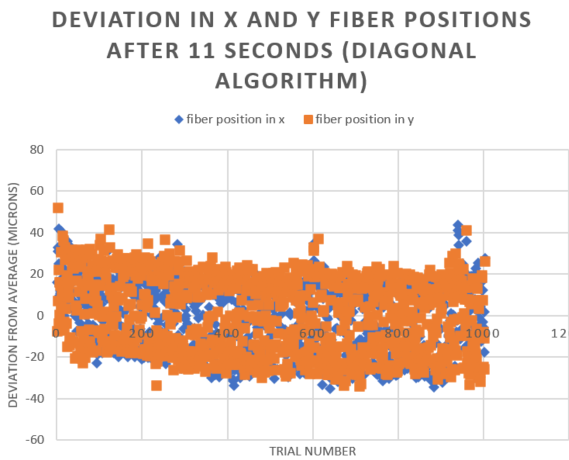

(b) Deviation from mean 11 seconds after the voltages were applied.

Figure 8: The deviation of the fiber from the mean upon 1005 trials of the diagonal reset procedure. The units for both graphs are microns in real space.

The behavior of the fiber tip immediately after the voltages were applied seem to be more erratic, at times jumping around almost 60 microns from the mean. In contrast, after 11 seconds, the fiber seems to have settled into place within 40 microns of the mean. At the end of the diagonal algorithm, the fiber is at the far corner of its range of motion – in position 5 when referring to figure 7. The final voltages that are applied across the electrodes is close to position nine, which means that the final movement in the Diagonal reset procedure is a large, sudden movement in the fiber, which would cause it to vibrate, explaining the erratic behavior seen in figure 8a and the settling into place seen in figure 8b. It is also possible that the blowers in the lab are contributing to the vibrations in the fiber. We examined the distribution in the plots above by making some histograms, which are shown below.

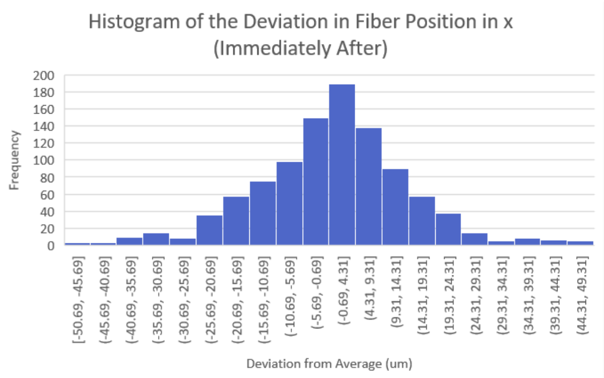

(a) Histogram showing the distribution of the deviation of fiber x positions from the mean upon doing the diagonal reset procedure. This is the data immediately after the voltages were applied.

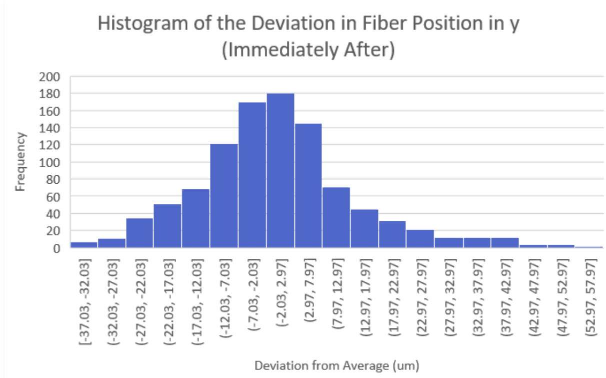

(b) Histogram showing the distribution of the deviation of fiber y positions from the mean upon doing the diagonal reset procedure. This is the data immediately after the voltages were applied.

Figure 9: We plotted histograms of the data shown in figure 8a to understand their distributions.

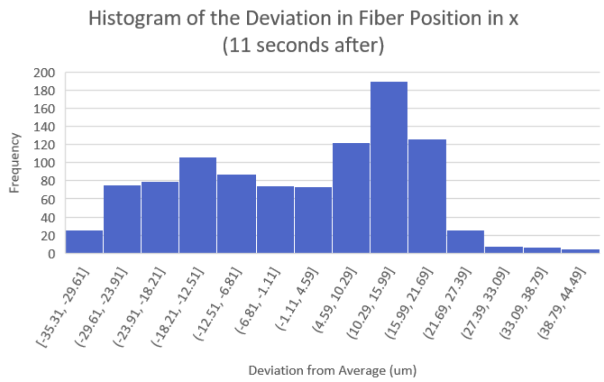

(a) Histogram showing the distribution of the deviation of fiber x positions from the mean upon doing the diagonal reset procedure. This is the data 11 seconds after the voltages were applied.

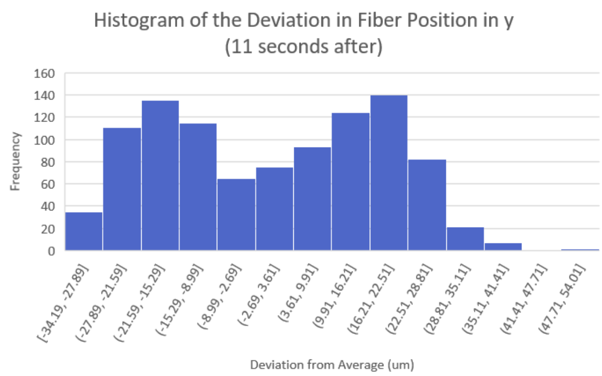

(b) Histogram showing the distribution of the deviation of fiber y positions from the mean upon doing the diagonal reset procedure. This is the data 11 seconds after the voltages were applied.

Figure 10: We plotted histograms of the data shown in figure 8b to understand their distributions.

The distributions in figure 9 look Gaussian, which suggest that the data is stochastic. However, in figure 10, the distributions no longer look Gaussian. This could be due to factors, such as creep, influencing the system, but we currently do not have a concrete explanation for this behavior.

The standard deviations of the final positions were calculated, and they are shown below.

Standard Deviation of Final Positions			
Immediate	Immediate	After 11 seconds	After 11 seconds
Standard Deviation in x (μm)	Standard Deviation in y (μm)	Standard Deviation in x (μm)	Standard Deviation in y(μm)
14.3 ± 0.3	14.3 ± 0.3	16.4 ± 0.4	18.1 ± 0.4

Since our goal is to be able to move the optical fiber to a given position within 10 μm, we want the standard deviation of the final positions to be within 10 μm. Looking at the table above, we see that while the values are calculated to be above our threshold, they are below 20 μm, which is a promising result and an excellent starting point.

5.2 Spiral Reset Procedure

The spiral reset procedure was repeated 1235 times and the final voltages applied across the north-south electrodes were 73 V and the east-west electrodes were 82 V. Below are the graphs that plotted the deviation of the fiber from the mean immediately after the voltages were applied and 11 seconds after.

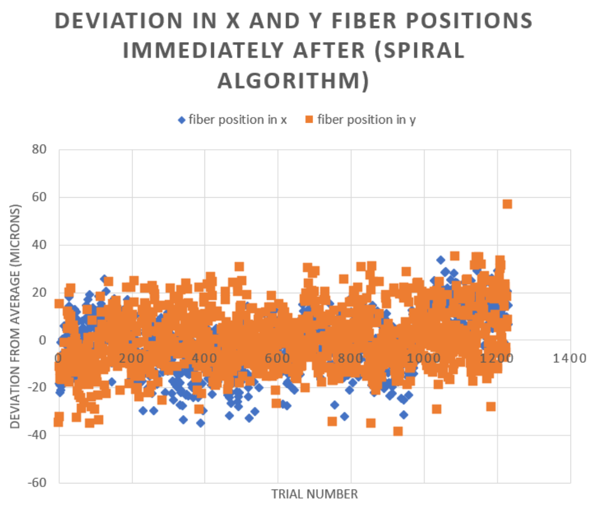

(a) Deviation from mean immediately after the voltages were applied.

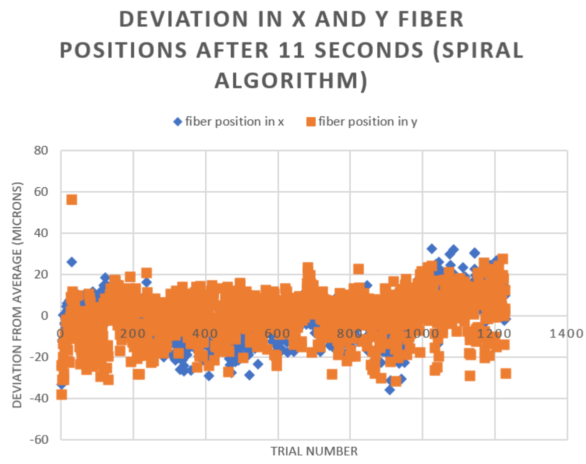

(b) Deviation from mean 11 seconds after the voltages were applied.

Figure 11: The deviation of the fiber from the mean upon 1235 trials of the spiral reset procedure. The units for both graphs are microns in real space.

Figure 11a and 11b are quite similar in that the final positions are contained within 40 microns of the mean. The last point on the graph in figure 11a as well as one of the first points on the graph in figure 11b are almost 60 microns from the mean. The likely explanation for this behavior is that upon making sure the experiment was running, I leaned on the table where the fiber positioner system is set up. Despite the system being set up securely, the fiber shakes when there is big movement in its surroundings, and that is reflected here. Again, we made some histograms to understand the distribution of the final fiber positions, shown in the plots below.

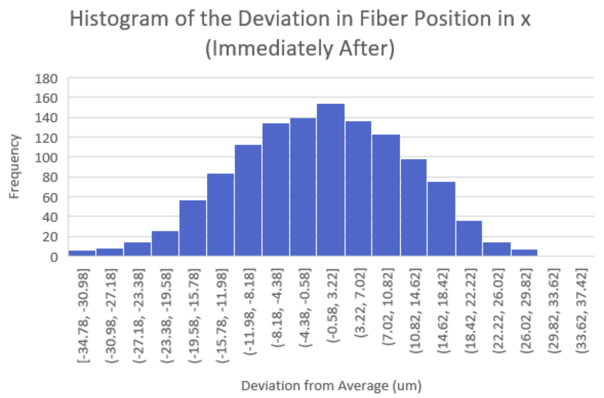

(a) Histogram showing the distribution of the deviation of fiber x positions from the mean upon doing the spiral reset procedure. This is the data immediately after the voltages were applied.

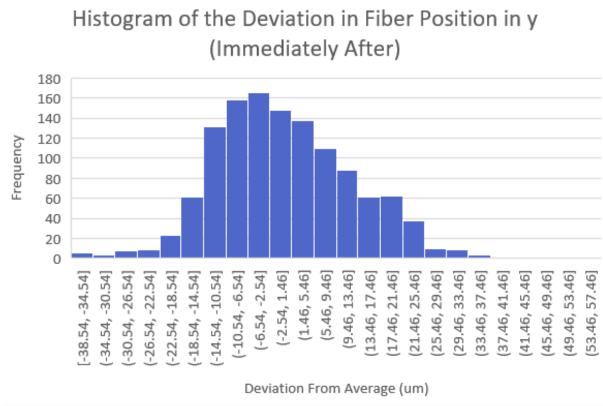

(b) Histogram showing the distribution of the deviation of fiber y positions from the mean upon doing the spiral reset procedure. This is the data immediately after the voltages were applied.

Figure 12: We plotted histograms of the data shown in figure 11a to understand their distributions.

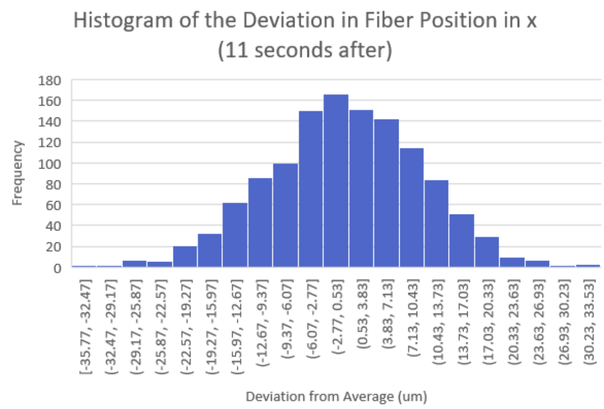

(a) Histogram showing the distribution of the deviation of fiber x positions from the mean upon doing the spiral reset procedure. This is the data 11 seconds after the voltages were applied.

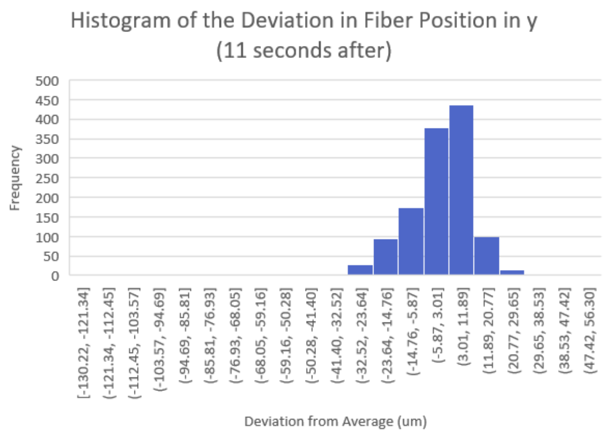

(b) Histogram showing the distribution of the deviation of fiber y positions from the mean upon doing the spiral reset procedure. This is the data 11 seconds after the voltages were applied.

Figure 13: We plotted histograms of the data shown in figure 11b to understand their distributions.

The four histograms above show a Gaussian distribution, which suggests that the data is stochastic. We have not yet determined why this data set has four Gaussian curves, while the data set for the diagonal reset procedure does not, and it would be an interesting phenomenon to explore further in the future.

The standard deviations of the final positions were calculated and they are shown in the table below.

Standard Deviation of Final Positions			
Immediate	Immediate	After 11 seconds	After 11 seconds
Standard Deviation in x (μm)	Standard Deviation in y (μm)	Standard Deviation in x (μm)	Standard Deviation in y(μm)
11.6 ± 0.2	12.1 ± 0.2	10.1 ± 0.2	11.0 ± 0.2

Though the standard deviations are not quite 10 μm, they are extremely close, especially after waiting for 11 seconds, another extremely promising result. When attempting to understand why the spiral reset procedure seems to produce better results than the diagonal reset procedure, it is important to note that the spiral algorithm ends in the center of the fiber's range of motion and the final voltages applied are 73 V across the north-south electrodes and 82 V across the east-west electrodes, which is not such a big movement compared to the diagonal reset procedure. This could explain why the standard deviations of the final positions for this reset procedure is closer to 10 μm.

5.3 Centered-Diagonal Reset Procedure

The results from both the diagonal reset procedure and the spiral reset procedure were promising, however we observed that the standard deviations of the final positions are closer to 10 μm when using the spiral reset procedure. We hypothesized that we can improve the results from the diagonal reset procedure if we slightly changed the diagonal algorithm to end in the center instead of the far corner of the fiber's dynamic range. Thus we decided to experiment with a modified version of the diagonal algorithm, where the fiber slowly moves to the center of its diagonal range of motion. Below are plots showing the deviation of the final positions of the fiber immediately after the voltages were applied and 11 seconds after. The voltages applied in the end are the same as what was applied for the diagonal and spiral reset procedures, which was 73 V across the north-south electrodes and 82 V across the east-west electrodes.

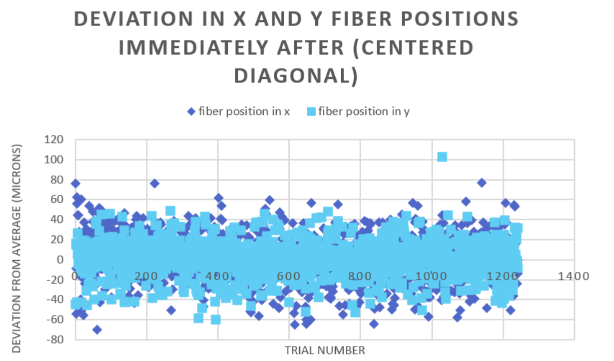

(a) Deviation from mean immediately after the voltages were applied.

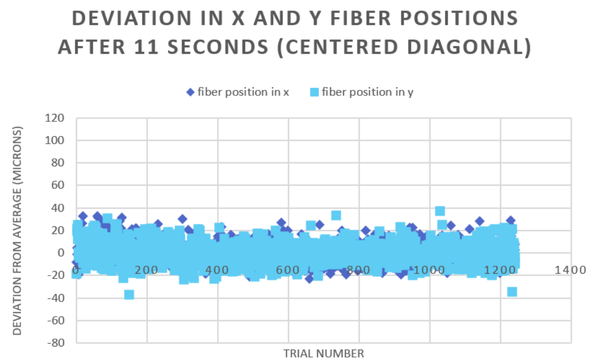

(b) Deviation from mean 11 seconds after the voltages were applied.

Figure 14: The deviation of the fiber from the mean upon 1242 trials of the centered-diagonal reset procedure. The units of both graphs are microns in real space.

There is an apparent difference in the two plots shown in figure 14. Figure 14a shows that the final positions are within 80 μm of the mean, whereas figure 14b show that the final positions are within 40 μm of the mean. The likely explanation for this result was that there was shakiness in the fiber directly after the final voltages were applied to the piezo and settled down after 11 seconds. When experimenting with extreme precision as we do here, it is not ideal for the fibers to shake as it is never quite certain when the fibers are done shaking. This is important to consider when choosing the best and appropriate procedure to eliminate hysteresis.

We made histograms for this data set as well, and they are shown below.

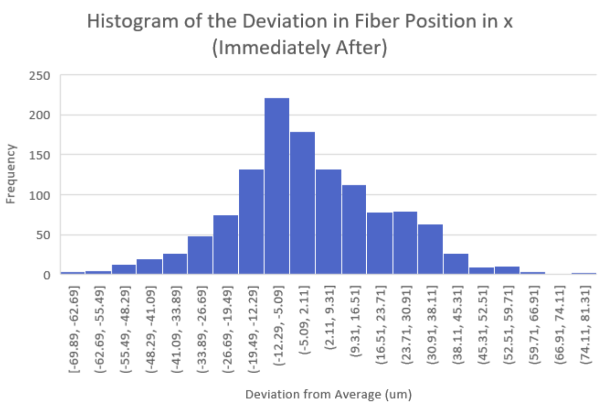

(a) Histogram showing the distribution of the deviation of fiber x positions from the mean upon doing the centered-diagonal reset. This is the data immediately after the voltages were applied.

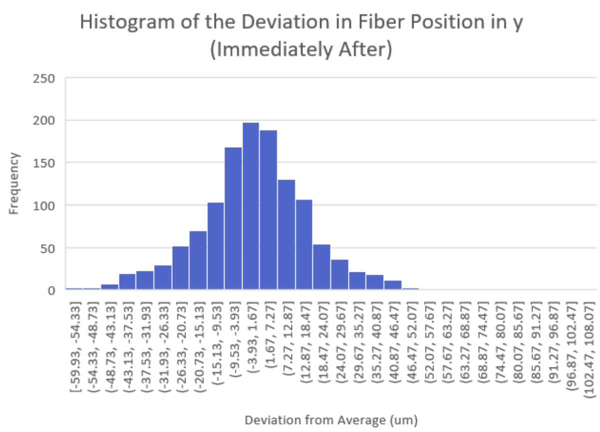

(b) Histogram showing the distribution of the deviation of fiber y positions from the mean upon doing the centered-diagonal reset. This is the data immediately after the voltages were applied.

Figure 15: We plotted this histograms of the data in figure 14a to understand their distributions.

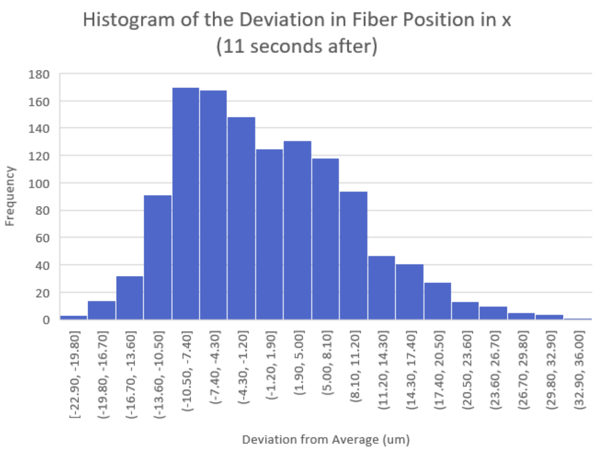

(a) Histogram showing the distribution of the deviation of fiber x positions from the mean upon doing the centered-diagonal reset. This is the data 11 seconds after the voltages were applied.

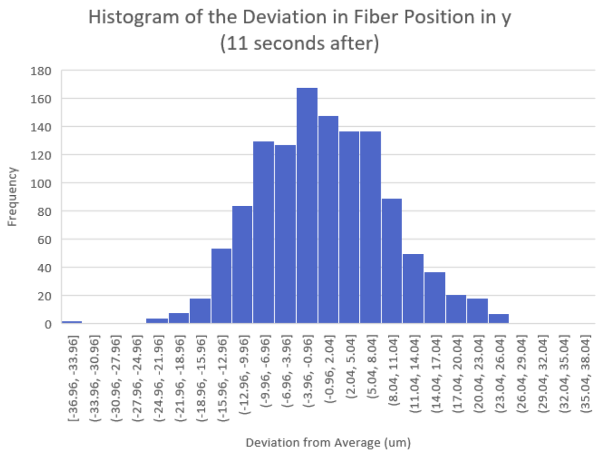

(b) Histogram showing the distribution of the deviation of fiber y positions from the mean upon doing the centered-diagonal reset. This is the data 11 seconds after the voltages were applied.

Figure 16: We plotted this histograms of the data in figure 14b to understand their distributions.

The distributions in figure 15a and 15b, as well as figure 16b look Gaussian, which show that the data is stochastic. Figure 16a has a distribution that resembles a bell curve, but shifted to the left a little bit. The data for the spiral reset procedure and this centered-diagonal reset exhibit more of a Gaussian distribution than the data for the diagonal reset. Though there are no concrete explanations behind these phenomenons, perhaps the symmetric nature of spiral and centered-diagonal algorithms play a part as well.

The standard deviations of the final positions were calculated and they are shown in the table below.

Standard Deviation of Final Positions			
Immediate	Immediate	After 11 seconds	After 11 seconds
Standard Deviation in x (μm)	Standard Deviation in y (μm)	Standard Deviation in x (μm)	Standard Deviation in y(μm)
22.1 ± 0.4	17.1 ± 0.3	9.4 ± 0.2	9.2 ± 0.2

This final reset procedure, which is much like a fusion of the diagonal and spiral reset procedure produced the lowest standard deviation. Although the standard deviations were on the higher end when looking at the data of the final positions immediately after the voltages were applied, after waiting for 11 seconds, we see that the standard deviations dipped below 10 μm, which is our goal!

5.4 3 x 3 Grid Mapping

Although it was incredible seeing the success of precisely returning the fiber tip to a single position in space, we must not forget there are many more positions that we must explore within and along the dynamic range of the fiber positioner system. Thus we have explored the nine positions labelled in figure 7; attempting to understand how precisely we can return to each of those positions, while utilizing the spiral reset for the first set of experiments and the diagonal reset for the next set. The results are shown below.

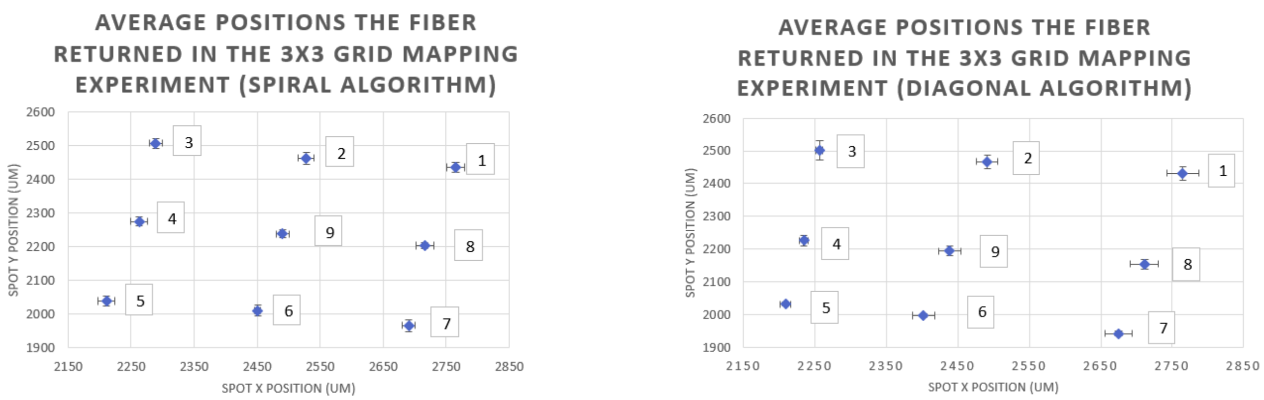

(a) Average positions the fiber returned using the spiral algorithm.

(b) Average positions the fibers returned using the diagonal algorithm.

Figure 17: Results of the grid experiments using two of the reset algorithms. The units of the graphs are microns in real space.

The 3x3 grid mapping experiment was repeated 32 times for each reset algorithm, and so forth the fiber was moved to each of the nine points 32 times. The blue points shown on the graphs above are the averages of those 32 positions recorded for each position. The horizontal error bars represent the standard deviations in the x direction and the vertical error bars represent the standard deviations in the y direction for each position. Similar to our previous experiments, it is our goal to return the optical fiber to each of those positions within a standard deviation of 10 μm.

The table below shows the standard deviations for the 3x3 grid experiment using the spiral algorithm.

3x3 Grid Mapping Experiment (Spiral Algorithm)			
Position number	Standard Deviation in x (μm)	Standard Deviation in y (μm)	Standard Deviation in Quadrature (μm)
1	14.4 $\pm$ 1.8	14.5 $\pm$ 1.8	20.4 $\pm$ 2.5
2	12.6 $\pm$ 1.6	17.7 $\pm$ 2.2	21.7 $\pm$ 2.7
3	10.8 $\pm$ 1.4	15.5 $\pm$ 1.9	18.9 $\pm$ 2.4
4	13.0 $\pm$ 1.6	13.7 $\pm$ 1.7	18.9 $\pm$ 2.3
5	13.2 $\pm$ 1.7	15.3 $\pm$ 1.9	20.2 $\pm$ 2.5
6	5.2 $\pm$ 0.7	16.6 $\pm$ 2.1	17.4 $\pm$ 2.2
7	9.8 $\pm$ 1.2	17.8 $\pm$ 2.2	20.3 $\pm$ 2.5
8	14.2 $\pm$ 1.8	9.9 $\pm$ 1.2	17.3 $\pm$ 2.2
9	9.8 $\pm$ 1.2	11.5 $\pm$ 1.4	15.1 $\pm$ 1.8

Looking at the standard deviations in quadrature, we see that it is lowest for position nine. This is not surprising because the spiral algorithm ends with the fiber in the center of its range of motion and position nine is extremely close to the center. Since there is minimal movement involved, there is little room for error. All other positions returned similar standard deviations in quadrature, even though the fiber must travel further to reach positions one, three, five, and seven, compared with positions two, four, six, and eight which are slightly closer to the center. This is a promising result because this shows that the spiral algorithm resets hysteresis to a similar degree no matter how far away the position is from the center. While the standard deviations in quadrature are not quite 10 μm, the values are extremely close to it and further exploration may reach such a result.

Below is a table that shows the standard deviations for the 3x3 grid experiment using the diagonal algorithm.

3x3 Grid Mapping Experiment (Diagonal Algorithm)			
Position number	Standard Deviation in x (μm)	Standard Deviation in y (μm)	Standard Deviation in Quadrature (μm)
1	22.0 $\pm$ 2.8	21.3 $\pm$ 2.7	30.6 $\pm$ 3.9
2	15.2 $\pm$ 1.9	21.3 $\pm$ 2.7	26.0 $\pm$ 3.3
3	4.8 $\pm$ 0.6	28.3 $\pm$ 3.5	28.7 $\pm$ 3.6
4	5.5 $\pm$ 0.7	15.9 $\pm$ 2.0	16.8 $\pm$ 2.1
5	7.1 $\pm$ 0.9	6.1 $\pm$ 0.8	9.3 $\pm$ 1.2
6	15.5 $\pm$ 1.9	5.2 $\pm$ 0.7	16.3 $\pm$ 2.0
7	19.1 $\pm$ 2.4	7.4 $\pm$ 0.9	20.5 $\pm$ 2.6
8	19.7 $\pm$ 2.5	15.1 $\pm$ 1.9	24.8 $\pm$ 3.1
9	16.1 $\pm$ 2.0	14.9 $\pm$ 1.9	21.9 $\pm$ 2.8

Looking at the column for the standard deviations in quadrature, we see that there is quite a difference in the values depending on the position number. Position five has the lowest standard deviation, and this is expected because position five is exactly where the diagonal algorithm ends. The closest positions to position five are position four, six, and nine, and they have a standard deviation in quadrature of 16.8 μm, 16.3 μm, and 21.9 μm, respectively. Some of the furthest positions from position five are positions one, two and eight and they have a standard deviation in quadrature of 30.6 μm, 26.0 μm, and 24.8 μm. These observations suggest that the positions closest to position five can return more precisely to their given locations and vice versa for the positions that are further from position five. This is not an appealing result because we need to be able to move the fibers to any position in space with a precision that is not compromised by how far away that position is from where the fiber previously was. It is possible that the large range in the standard deviations are caused due to the diagonal algorithm ending in one corner of the dynamic range instead of the center. To confirm this hypothesis, this experiment should be repeated with the centered-diagonal algorithm as well.

6 Conclusions and Future Outlook

Throughout this experiment, we explored three algorithms to mitigate hysteresis. We began by attempting to understand how well the reset procedures can precisely return the fiber tip to one specific position within the dynamic range of the fiber positioner system. We found that all three reset procedures were able to return the fiber tip to within 20 μm, and we saw an incredible success with the centered-diagonal reset procedure, where we were able to return the fiber tip to within 10 μm. However, being able to precisely return to a single position is not nearly enough, as there are numerous more positions waiting to be explored. So forth, in the next series of experiments we explored nine more positions along and within the dynamic range of our system. We found that the fiber returned to each of these positions within 25 μm, which is an extremely promising result that we hope to improve in the future.

The initial set up that we had been working with had a malfunctioning part, however it was difficult to diagnose exactly what the issue was when there appeared to be nothing faulty in the circuit boards that we were working with. After extensive problem solving, we decided to create a whole new set up from scratch and pick up the research from there. At times I felt frustrated and ashamed that my research was not moving as planned and I was falling behind from all that I wanted to experiment with, but there was so much to be learned from research not going well. Without a doubt, the greatest lesson from this thesis is the power of overcoming challenges.

The next steps of this project is to experiment with more than one fiber. We recently created a new set up with three fibers and since our long term plan is to have a system with 50,000 fibers, this would be an excellent step in dealing with a multi-fiber system, and making sure the experiments discussed in this thesis work produce similar results. Taking the 3x3 grid experiment further and exploring with more positions would also be great in establishing a first map between the voltages applied to the piezo and the positions of the fiber tip. Creep is the other inherent property of the piezos that we must learn to mitigate, and this would be integral in making this spectroscopic telescope a reality.

References

[1] Abdurro'uf et al. "The Seventeenth Data Release of the Sloan Digital Sky Surveys: Complete Release of MaNGA, MaStar, and APOGEE-2 Data". In: 259.2, 35 (Apr. 2022), p. 35. DOI: 10.3847/1538-4365/ac4414. arXiv: 2112.02026 [astro-ph.GA].

[2] Lauren Anderson et al. "The clustering of galaxies in the SDSS-III Baryon Oscillation Spectroscopic Survey: baryon acoustic oscillations in the Data Releases 10 and 11 Galaxy samples". In: *Monthly Notices of the Royal Astronomical Society* 441.1 (Apr. 2014), pp. 24–62. DOI: 10.1093/mnras/stu523. URL: https://doi.org/10.1093%2Fmnras%2Fstu523.

[3] Kevan Hashemi. *Movement of the Fiber Tip Perpendicular to the Focal Plane.* 2022.

[4] Alexis Hill et al. *The Maunakea Spectroscopic Explorer Book 2018.* 2018. DOI: 10.48550/ARXIV.1810.08695. URL: https://arxiv.org/abs/1810.08695.

[5] David R. Law et al. "THE DATA REDUCTION PIPELINE FOR THE SDSS-IV MaNGA IFU GALAXY SURVEY". In: *The Astronomical Journal* 152.4 (Sept. 2016), p. 83. DOI: 10.3847/0004-6256/152/4/83. URL: https://doi.org/10.3847%2F0004-6256%2F152%2F4%2F83.

[6] Daniela Leitner et al. *Dark Energy Spectroscopic Instrument (DESI) Fiber Positioner Production.* 2018. DOI: 10.48550/ARXIV.1807.09907. URL: https://arxiv.org/abs/1807.09907.

[7] Philip Massey and Margaret Hanson. "Astronomical Spectroscopy". In: *Planets, Stars and Stellar Systems. Volume 2: Astronomical Techniques, Software and Data* (Oct. 2010). DOI: 10.1007/978-94-007-5618-2_2.